Study of the Amorphous Phase in Semicrystalline Poly(ethylene terephthalate) via Physical Aging

Jun Zhao, Jijun Wang, Chaoxu Li, and Qingrong Fan*

State Key Laboratory of Polymer Physics & Chemistry, Center for Molecular Science, Institute of Chemistry, Chinese Academy of Sciences, Beijing 100080, P. R. China

Received July 26, 2001; Revised Manuscript Received January 8, 2002

ABSTRACT: Amorphous phase in semicrystalline poly(ethylene terephthalate) (PET) was investigated via its physical aging behavior. It was found that when the degree of crystallinity (f_c^w) was within a definite range, there were dual amorphous regions with quite different characters in semicrystalline PET: free amorphous region and constrained amorphous region. Both lower and upper limits of the f_c^w range increased with increasing crystallization temperature (T_c) for semicrystalline samples crystallized from the glassy state. The dual amorphous regions showed as dual tan δ loss peaks in dynamic mechanical thermal analysis (DMTA) curves, and when the samples had been physically aged, there were dual endothermic physical aging peaks appearing in the glass transition region of differential scanning calorimetry (DSC) traces. With the proceeding of physical aging, some of the free amorphous region evolved into the constrained amorphous region due to the reduced mobility of chain segments produced by physical aging. The whole amount of the amorphous phase, however, was kept almost constant during the whole process of physical aging. Amorphous phase in semicrystalline samples crystallized from the melt was also discussed.

Introduction

Poly(ethylene terephthalate) (PET) is one of the most commercially important polyesters with excellent thermal and chemical resistance and mechanical performance.[1,2] It finds widespread uses in fibers, films, and other engineering components. Because of its high melting temperature (T_m) and glass transition temperature (T_g), and in particular its moderate crystallization rate, a great variety of microstructures can be easily developed. Size, shape, and perfection of crystallites, volume fractions of different phases, and orientation of molecular chains all can be varied by changing process conditions of PET. Many researchers have investigated its crystalline phase,[1,3−9] but less attention was paid to its amorphous phase and many aspects have not yet been fully clarified.[2,10−13]

At temperatures below but close to the T_g, amorphous polymers are in thermodynamic nonequilibrium. Their physical properties such as specific volume, enthalpy, and entropy are greater than the equilibrium values. Thus, these properties decrease toward the equilibrium values. Coupled with these changes, mechanical properties, dielectric properties, and microstructure of the samples also vary. This process is generally called structural relaxation or physical aging.[14,15] In previous years, physical aging was experimentally studied mainly by measuring volume relaxation of the samples via dilatometry,[16−18] but later more studies were about enthalpy relaxation via differential scanning calorimetry (DSC), which was convenient, sensitive, and highly reproducible.[19−25] One of the earlier studies by Petrie established the equivalence between the energy absorbed during the heating run through the glass transition region and the enthalpy lost during the physical aging.[19]

* To whom correspondence should be addressed. Telephone: +86 10 62563065. Fax: +86 10 62559373. E-mail: qrfan@pplas.icas.ac.cn.

Infrared (IR) spectroscopy also can be used to study the crystallization, orientation, and physical aging of PET by monitoring the conformation changes.[3,5,26,27] Generally, 973 and 898 cm^{-1} bands were assigned to the trans and *gauche* conformations of the ethylene glycol moiety along the PET chain, respectively,[3,10,12,26,28,29] while various bands such as 795, 875, 1058, and 1578 cm^{-1} were all used as internal references.[3,12,28,29] It was found that the amount of gauche conformation increased with the proceeding of physical aging.[10,29] Similar results were also obtained in our laboratory by assigning 1340 and 1370 cm^{-1} bands to the trans and gauche conformations, respectively.[30−33]

Physical aging in semicrystalline polymers was first studied for polypropylene (PP) films.[34] The physical aging was found to be able to occur at temperatures above the T_g and remarkably similar to that in wholly amorphous polymers. To explain these phenomena, several models were put forward.[17,35−41] One of the best known is the model of "extended glass transition".[17,36] According to the model, crystallites in semicrystalline samples disturb the amorphous phase and reduce the mobility of molecular segments. The reduction will reach its maximum in the immediate vicinity of the crystallites, and only at large distances from the crystallites will the properties of amorphous phase become equal to those of the wholly amorphous samples. The main consequence of this immobilization is that the glass transition will be extended to higher temperatures. Above T_g of the wholly amorphous samples, some parts of the amorphous phase are rubbery, others are glassy, and still other parts will just be passing their own glass transition. Concerning physical aging, the model predicted the following: below the T_g, amorphous phase would be completely glassy and suffered from the same physical aging effects as the wholly amorphous samples. Above the T_g, some parts of the amorphous phase of the semicrystalline polymers were still glassy. So, physical aging would persist at temperatures above the T_g, a

10.1021/ma011333z CCC: $22.00
Published on Web 03/08/2002

behavior not exhibited by wholly amorphous polymers.

Some literature reported that when the f_c^w of semicrystalline PET was within a certain range, there were dual endothermic physical aging peaks appearing in the T_g region of DSC traces.[38,40,42] The dual peaks were assigned to the enthalpy relaxation of dual amorphous regions: the interspherulitic amorphous region outside the spherulites and the interlamellar amorphous region inside the spherulites.[38,40]

Our previous paper has briefly reported that only when the f_c^w was in a definite range, the dual peaks appeared, and both lower and upper limits of the f_c^w range increased with increasing crystallization temperature (T_c).[43] In this paper, the existence of dual amorphous regions will be further confirmed via dynamic mechanical thermal analysis (DMTA). Wider range of T_c and various physical aging temperatures (T_{pa}) will also be employed to study characters of the dual amorphous regions. The structural changes in amorphous phase occurring during physical aging will also be discussed.

Experimental Section

Materials. Amorphous PET films were kindly supplied by Beijing Plastics Co. The samples had a thickness of ca. 0.15 mm, a viscosity-average molecular weight of ca. 1.63×10^4, a density of ca. 1.335 g cm^{-3}, which means that samples were wholly amorphous, and an optical birefringence of ca. 6×10^{-4}, which means that there was no orientation. Measurements by both DSC and wide-angle X-ray diffraction (WAXD) also showed that the samples were wholly amorphous.

Heat Treatments. As-received PET films were cut into equal rectangles with a size of ca. 20.0 × ca. 5.0 mm (for DMTA measurements) or circles with a diameter of ca. 5.7 mm (for DSC measurements). They were held in an oven in nitrogen atmosphere at 300 ± 0.5 °C (ca. 45 °C above their T_m of ca. 255 °C) for 5 min to completely eliminate their thermal history. Then some samples were quenched in air to room temperature of ca. 25 °C. It has proved that there was no crystallization induced by this process. Subsequently, these quenched samples crystallized isothermally in an oven in nitrogen atmosphere at various temperatures between 85 and 130 °C for different time to obtain different f_c^w. There were also some samples which were quenched directly at 100 °C min^{-1} in the oven to predetermined temperatures above 200 °C and then held for different time to obtain different f_c^w. Then all the semicrystalline samples crystallized from the glassy state or the melt were physically aged in an oven in nitrogen atmosphere at various temperatures between 63 and 78 °C for different periods of time. At last they were taken out and stored in a desiccator before other measurements.

f_c^w Measurements. Density of semicrystalline PET (ρ) was measured at 25 ± 0.1 °C by using a density gradient tube filled with carbon tetrachloride and *n*-heptane. The density gradient tube was calibrated by suspending glass beads with known densities. f_c^w (apparent weight percent degree of crystallinity) of the samples was calculated by taking the density of wholly amorphous samples (ρ_a) to be 1.335 g cm^{-3} and that of perfect PET crystalline lamellae (ρ_c) to be 1.455 g cm^{-3}.[28,38,39,44,45] Then

$$f_c^w = (\rho_c(\rho - \rho_a))/(\rho(\rho_c - \rho_a)) \times 100\% \quad (1)$$

DSC Measurements. Physically aged samples of ca. 5.0 mg were sealed in aluminum pans and their thermal properties were measured by using a TA2910 DSC. Indium and tin were employed for the temperature calibration, the heat capacity was evaluated with respect to sapphire as a standard, and a nitrogen gas purge with a flux of ca. 30 mL min^{-1} was used to prevent oxidative degradation of samples during the heating run. The rate of the heating run in DSC was 10 °C min^{-1}, unless otherwise specified.

DMTA Measurements. DMTA measurements were performed in a Rheometric Scientific DMTA IV at a frequency of 1 Hz and a heating rate of 5 °C min^{-1}. Samples were stretched by an initial stress of 0.2 N. Dynamic modulus ($G^* = G' + iG''$) and loss tangent ($\tan \delta = G''/G'$) were obtained.

Polarizing Optical Microscopy (POM). Crystalline morphology and spherulites size of the semicrystalline samples were measured at room temperature by using an Olympus BH-2 POM equipped with a Mettler FP-52 hot stage.

Results and Discussion

Our previous paper has reported that when the semicrystalline poly(ethylene terephthalate) (PET) samples with a moderate degree of crystallinity (f_c^w) had been physically aged, there were dual endothermic peaks appearing in the glass transition temperature (T_g) region of their differential scanning calorimetry (DSC) traces.[43] As shown in Figure 1, parts a and b, when the f_c^w of semicrystalline samples was very low (even to be 0, for wholly amorphous samples) or fairly high (e.g. ca. 39%, obtained by isothermal crystallization at 130 °C for 7.5 min), there was only a single endothermic physical aging peak appearing in the T_g region, and the peak shifted to higher temperatures with increasing physical aging time (t_{pa}). As shown in Figure 1c, however, when the f_c^w of semicrystalline samples was between these two extreme cases (e.g. ca. 17%, obtained by isothermal crystallization at 120 °C for 7.0 min), there were dual endothermic physical aging peaks appearing in the T_g region, and both the dual peaks shifted to higher temperatures with increasing t_{pa}.

By comparing Figure 1c with Figure 1, parts a and b, respectively, it can be seen that the lower endothermic peak had almost the same temperature range as the single peak in wholly amorphous samples, while the upper peak had almost the same range as that in semicrystalline samples with the fairly high f_c^w. Besides, the lower peak had a shape similar to that of the single peak in wholly amorphous samples, while the upper peak had a shape similar to that in semicrystalline samples with the fairly high f_c^w. Third, both the lower peak and the single peak in wholly amorphous samples appeared after a t_{pa} of only ca. 0.375 h, while both the upper peak and the single peak in semicrystalline samples with the fairly high f_c^w became visible after a t_{pa} of ca. 1.5 h.

Physical aging in polymers occurs in the amorphous phase and it can enhance the DSC response at the glass transition.[14,15,34,36] Thus, characters of amorphous phase can be obtained by studying its physical aging behavior.[38,40,41,46] It is well-known that there was only free amorphous region in wholly amorphous samples and only constrained amorphous region in semicrystalline samples with the fairly high f_c^w.[38,40] Therefore, according to the comparison of Figure 1c with Figure 1, parts a and b as mentioned above, it seems plausible to conclude that, in the semicrystalline samples showing the dual physical aging peaks, there were dual amorphous regions: free amorphous region and constrained amorphous region.

When the dual endothermic physical aging peaks appeared, there was still an exothermic cold crystallization peak appearing in DSC traces. In fact, because there was no orientation in the samples, the cold crystallization temperature (T_{cc}) was fairly high (ca. 137 °C, measured by DSC at 10 °C min^{-1}, for wholly amorphous samples). T_{cc} of semicrystalline samples with a fairly high f_c^w was still well above the temperature

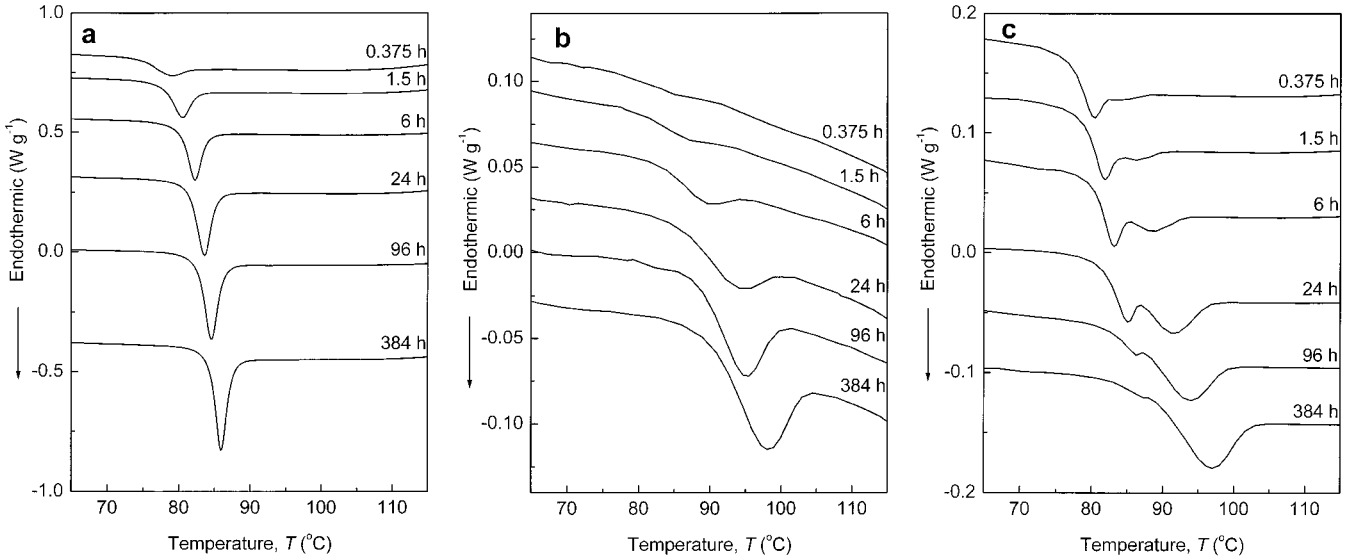

Figure 1. DSC traces of amorphous PET (a), semicrystalline samples with a f_c^w of ca. 39% (obtained by isothermal crystallization at 130 °C for 7.5 min) (b), and semicrystalline samples with a f_c^w of ca. 17% (obtained by isothermal crystallization at 120 °C for 7.0 min) (c) physically aged at 68 °C for different t_{pa} indicated beside each curve.

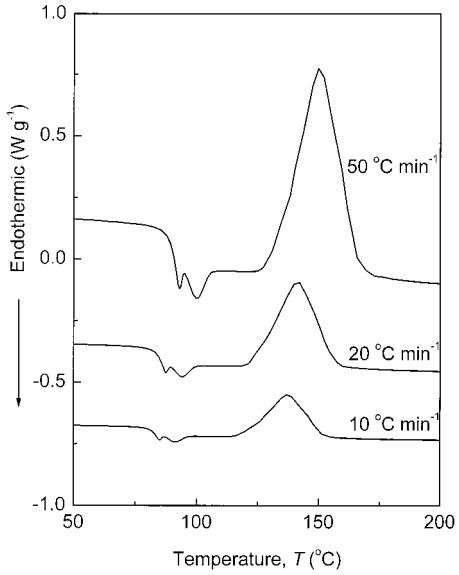

Figure 2. DSC traces of semicrystalline PET with a f_c^w of ca. 17% (obtained by isothermal crystallization at 120 °C for 7.0 min) physically aged at 68 °C for 24 h at different heating rates of DSC indicated beside each curve.

range of the dual endothermic peaks. Very low T_{cc}, even as low as the T_g, can be found in highly oriented PET fibers, where the high orientation plays an important role in accelerating the cold crystallization.[47]

As shown in Figure 2, both the dual endothermic physical aging peaks and the exothermic cold crystallization peak shifted to higher temperatures with increasing heating rate of DSC. It can be seen that the shape of all three peaks was preserved. Besides, measurement of the density showed that there was no further crystallization occurring in the temperature range of the dual peaks when samples were heated in DSC. Therefore, it can be concluded that there was no cold crystallization involved in the dual endothermic physical aging peaks. Similar experimental results and theoretical explanations have been well documented.[35,38−42,48,49]

Dynamic mechanical measurements are known to be sensitive to the glass transition and other secondary transitions of polymers.[38,39,44,50] Figure 3 presents DMTA curves of the three different samples as mentioned in Figure 1. It can be seen that for both wholly amorphous samples and semicrystalline samples with the fairly high f_c^w, there was only a single tan δ loss peak related to the glass transition. However, for semicrystalline samples with the intermediate f_c^w, there were dual tan δ loss peaks related to the glass transition. This is a direct evidence of dual amorphous regions. Similar experimental results can be found in others' research.[38]

By comparing Figure 3c with Figure 3, parts a and b, respectively, it can be seen that the lower loss peak had almost the same temperature range as the single peak in wholly amorphous samples, while the upper peak had almost the same range as that in semicrystalline samples with the fairly high f_c^w. Besides, the lower peak had a shape similar to that of the single peak in wholly amorphous samples, while the upper peak had a shape similar to that in semicrystalline samples with the fairly high f_c^w. Therefore, it also can be concluded that there were both a free amorphous region and a constrained amorphous region in semicrystalline samples with the moderate f_c^w.

In fact, the existence of dual amorphous regions in semicrystalline PET has also been confirmed by using small-angle X-ray diffraction (SAXD), electron microscopy (EM), and thermally stimulated current (TSC) techniques.[35,41]

Our previous paper has reported that the dual endothermic physical aging peaks appeared only when the f_c^w of samples was in a definite range, and both lower and upper limits of the f_c^w range increased with increasing T_c for crystallization at temperatures between 100 and 130 °C from the glassy state.[43] Our experiments showed that this law could be extended to lower crystallization temperatures. As shown in Figure 4a, when f_c^w of samples was below the lower limit, there was a single endothermic peak similar to that shown in Figure 1a, while when f_c^w was above but close to the upper limit, there was a single endothermic peak similar to that shown in Figure 1b. Only when f_c^w was between the lower and upper limits, dual endothermic peaks similar to those shown in Figure 1c could be obtained.

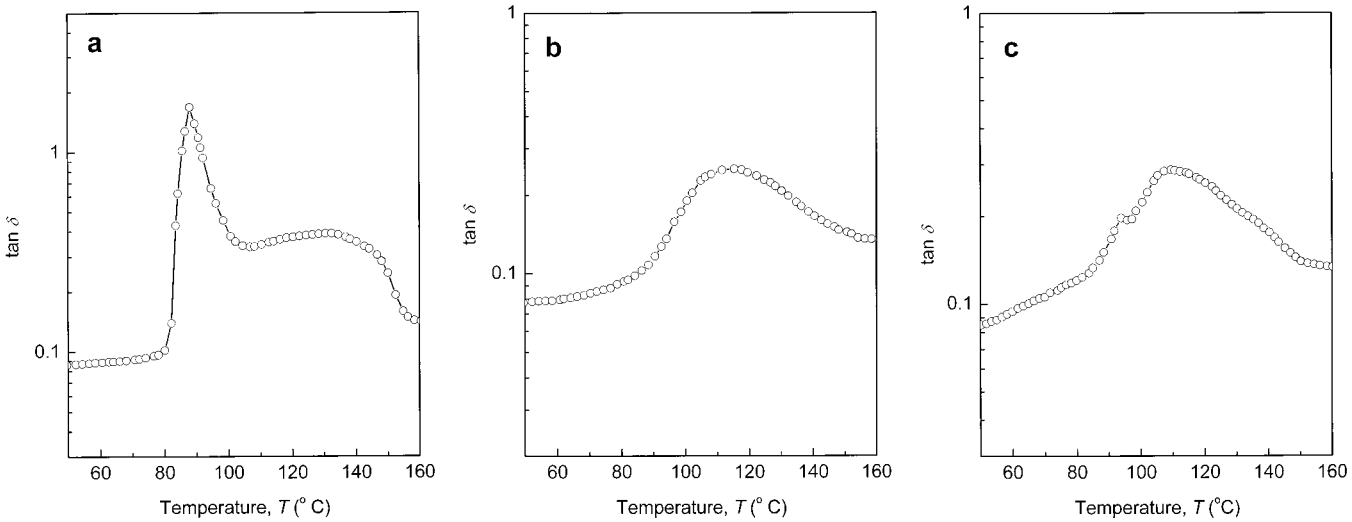

Figure 3. DMTA curves of amorphous PET (a), semicrystalline samples with a f_c^w of ca. 39% (obtained by isothermal crystallization at 130 °C for 7.5 min) (b), and semicrystalline samples with a f_c^w of ca. 17% (obtained by isothermal crystallization at 120 °C for 7.0 min) (c).

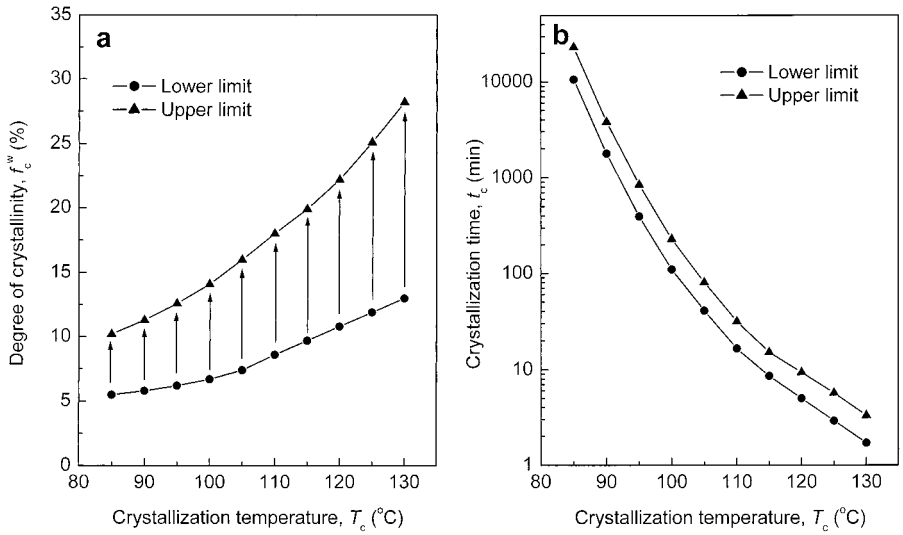

Figure 4. Range of f_c^w (a) and t_c (b) corresponding to different T_c (dual endothermic physical aging peaks appeared when the semicrystalline samples were between the lower and upper limits).

Figure 4b presents the range of crystallization time (t_c) to get the f_c^w range shown in Figure 4a. It can be seen that t_c decreased with increasing T_c although the required f_c^w increased. For crystallization at 85 °C, t_c of ca. 10 600 and ca. 23 200 min were needed to reach the f_c^w values of ca. 5.5% and ca. 10.2%, respectively, while for crystallization at 130 °C, f_c^w values of ca. 13.0% and ca. 28.2% needed a t_c of only ca. 1.7 and ca. 3.3 min, respectively.

No results were obtained for the crystallization at lower temperature between 85 °C and the T_g (ca. 78 °C, measured by DSC at 10 °C min^{-1}) due to the too long t_c even if the crystallization still occurred. For unoriented wholly amorphous PET, it was reported that there was a temperature interval above but close to the T_g, at which there was only molecular rearrangement but no detectable crystallization.[51] For higher T_c above 130 °C, no results about the f_c^w range for the appearance of dual endothermic physical aging peaks were obtained due to the too high crystallization rate, which made it difficult to control the f_c^w of semicrystalline samples.

Constraint that the crystallites exerted on the amorphous phase is the most important factor that determined characters of the amorphous phase.[17,36] No such constraint existed in wholly amorphous samples, and the constraint was very weak in semicrystalline samples with a very low f_c^w. So, only free amorphous region existed in them. However, the constraint was very strong in semicrystalline samples with a fairly high f_c^w. So, only constrained amorphous region existed in them. Only in semicrystalline samples with the intermediate f_c^w, the constraint was moderate and both free amorphous region and constrained amorphous region coexisted in the samples.

Both Struik and Hay pointed out that such constraint depended on not only f_c^w of the semicrystalline samples but also the morphology, especially the size of the crystallites.[17,36,50] At higher T_c, nucleation rate was lower, while segmental diffusion rate was higher, so the nuclei was fewer but their size was larger.[52] Consequently, crystallites were more perfect and had a larger size. Thus, for the same f_c^w, the amorphous region had higher volume fraction and the constraint that crystallites exerted on the amorphous phase was weaker. Therefore, to get almost the same constraint, higher f_c^w was needed for higher T_c as shown in Figure 4a.

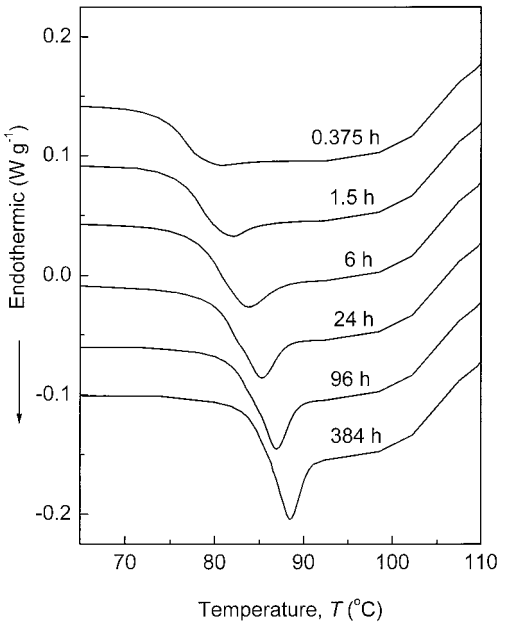

Figure 5. DSC traces of semicrystalline PET with a f_c^w of ca. 17% (obtained by isothermal crystallization at 220 °C for 9.0 min) physically aged at 68 °C for different t_{pa} indicated beside each curve.

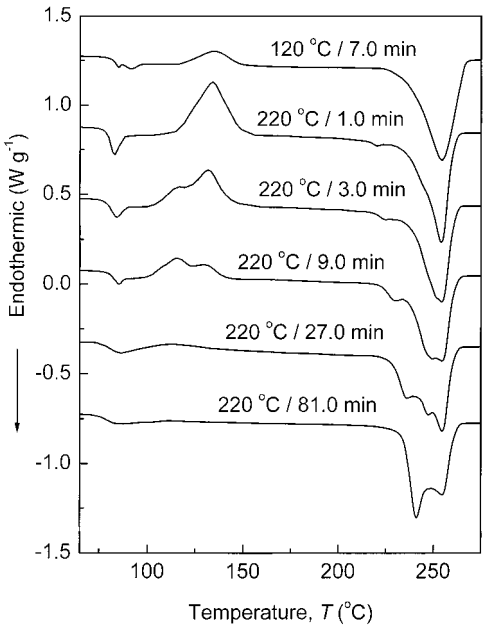

Figure 6. DSC traces of semicrystalline PET (obtained by isothermal crystallization at 120 or 220 °C for different t_c indicated beside each curve) physically aged at 68 °C for 24 h.

In our experiments, semicrystalline samples with the same f_c^w of ca. 12% were obtained by isothermal crystallization at 85 and 130 °C, respectively. The former was found to be much more transparent than the latter. In the former, spherulites could hardly be found by polarizing optical microscopy (POM) due to their too small size, while in the latter, spherulites with average diameter of ca. 2 μm could be found. Similar results can be found in others' research.[35,38,53,54]

In our experiments, the crystallization rate of wholly amorphous PET reached its maximum at ca. 168 °C. The crystallization at 220 °C had a similar rate to that at 120 °C. Figure 5 shows the DSC traces of semicrystalline PET samples with the same f_c^w of ca. 17% as that of the samples in Figures 1c and 3c (obtained by isothermal crystallization at 220 °C for 9.0 min) physically aged at the same physical aging temperature (T_{pa}) of 68 °C as that in Figure 1c. It can be seen that there was only a single endothermic physical aging peak appearing in the T_g region. Both the T_p and the shape showed that the peak could be assigned to physical aging of the free amorphous region. According to the law shown in Figure 4a, for the T_c of 220 °C, dual endothermic peaks should appear at higher f_c^w if they really appeared. But such dual peaks were never found in our experiments. The reason can be found from Figure 6. For crystallization at 120 °C, there was only a single exothermic cold crystallization peak appearing at ca. 135 °C after a t_c of 7.0 min. However, for crystallization at 220 °C, there were dual cold crystallization peaks appearing at lower temperatures and the dual exothermic peaks shifted to lower temperature with increasing t_c. They decreased to ca. 116.7 and ca. 131.7 °C after a t_c of 9.0 min. The lower exothermic cold crystallization peak will overlay the upper endothermic physical aging peak if the upper peak really exists. In other words, whether there were dual amorphous regions in such semicrystalline samples cannot be judged by DSC traces, and other measurements must be employed. It was ever reported that crystallization at low-temperature such as 100 and 105 °C from the glassy state also resulted in dual cold crystallization peaks in DSC traces,[55] but such phenomena were never found in our samples.

As shown in Figure 1c, both the dual peaks shifted to higher temperatures with increasing t_{pa}, so did intensity of the upper peak (ΔH^U). Intensity of the lower peak (ΔH^L), however, first increased but then (after a critical t_{pa}, t_{pa}^c) decreased. Figure 7 presents DSC traces of the same samples as in Figure 1c physically aged at various temperatures. It can be seen that the dual peaks for the T_{pa} of 63 and 73 °C also followed the same evolution laws as mentioned above. However, for the T_{pa} of 78 °C, the lower peak disappeared after a very short t_{pa} and the upper peak was wider than that at other T_{pa}. At T_{pa} of 78 °C, which has been within the T_g region, the free amorphous region cannot remain in the glassy state any longer, so only the constrained amorphous region existed. Thus, there was almost just the upper peak visible alone. In fact, for the different T_c and T_{pa}, as long as dual endothermic physical aging peaks appeared, all of them followed such evolution laws. By comparison Figure 7 with Figure 1c, it can be seen that t_{pa}^c decreased and the upper peak appeared earlier with increasing T_{pa}, which showed that the rate of physical aging was higher with increasing T_{pa}.[42]

During physical aging, there was an increase of density of less than 0.4%, which depended on the T_{pa}. For the T_{pa} of 68 °C, the typical increase of density was ca. 0.1%, which was a typical density change produced by physical aging.[15,17] Therefore, it seems plausible to assume that there was no further crystallization occurring during physical aging and the whole amount of amorphous phase in the semicrystalline samples kept constant. In fact, there was no evidence of further crystallization occurring during physical aging no matter samples were amorphous or semicrystalline.[10,11,29,39,44,56]

It should be pointed out that in our calculation of f_c^w, density of wholly amorphous samples (ρ_a) was assumed to be constant as shown in eq 1. Thus, the obtained f_c^w was just an apparent value.[28] Because there was no

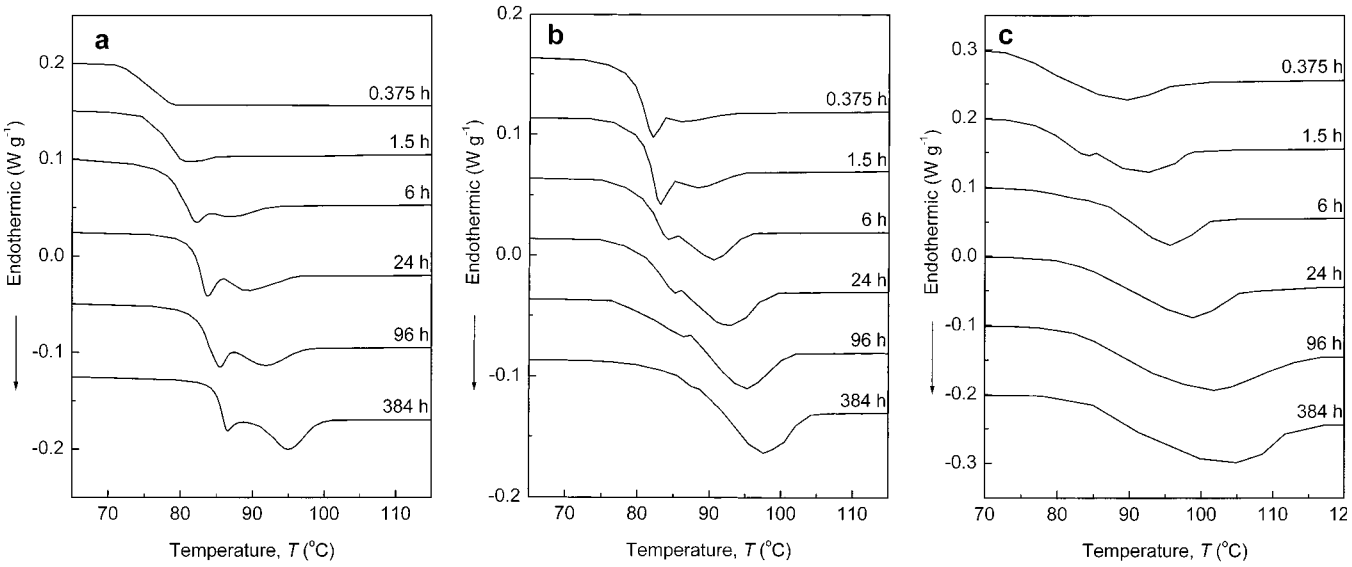

Figure 7. DSC traces of semicrystalline PET with a f_c^w of ca. 17% (obtained by isothermal crystallization at 120 °C for 7.0 min) physically aged at 63 (a), 73 (b), and 78 °C (c) for different t_{pa} values indicated beside each curve.

orientation in our samples and there was no further crystallization during physical aging as mentioned above, such an assumption did not affect our analysis of the experimental results.

It is well-known that, when the amount of amorphous region kept constant, increasing extent of the physical aging with increasing t_{pa} would make intensity of the endothermic peak (ΔH) increase. Thus, the fact that ΔH^L first increased but then decreased after a t_{pa}^c can be explained only by considering a decrease of amount of the free amorphous region with increasing t_{pa}. It seems plausible to assume that amount of the free amorphous region in the semicrystalline samples decreased from beginning of the physical aging. Coupled with this decrease, the amount of the constrained amorphous region increased due to the constant whole amount of the amorphous phase.

ΔH was determined mainly by two factors: the extent of physical aging and the amount of amorphous region. For the constrained amorphous region, both the factors increased during the whole process of physical aging, so ΔH^U increased continuously. For the free amorphous region, however, the former increased, while the latter decreased, so the change of ΔH^L was determined by both of them. In the early stage of physical aging, increase of the former was dominant, so ΔH^L increased. In the late stage, however, decrease of the latter was dominant, so ΔH^L decreased. Therefore, ΔH^L reached its maximum at the t_{pa}^c.

During physical aging, both the enthalpy and the volume of the samples decreased, so the mobility of chain segments also decreased.[14,15,17] That is to say, besides the constraint that crystallites exerted on the amorphous phase, physical aging also produced some constraint on it. Our experiments showed that tan δ loss peaks for all the samples shown in Figure 3 shifted to higher temperatures with increasing t_{pa}, which means that physical aging really produced some constraint on the amorphous phase.[39,44] Increasing constraint gave more amorphous phase characters of constrained amorphous region. Therefore, some of the free amorphous region evolved into the constrained amorphous region.

Most of the models of semicrystalline polymers accepted the concept of "dual amorphous regions" (free amorphous region and constrained amorphous region).[17,35,36,38−41,57] In some models, amorphous phase outside the spherulites was assigned to the free amorphous region and that inside the spherulites to the constrained region.[35,38−41] In the model of "extended glass transition",[17,36] however, the amorphous phase was divided only by its distance from the crystallites. Boyer pointed out that dual amorphous regions were fairly common in semicrystalline polymers and multiple amorphous regions were even more natural.[48,49] Only the model of "extended glass transition" allowed change of the amount of each amorphous region under the condition of constant whole amount of amorphous phase. Therefore, the model of "extended glass transition" seems to be more suitable for our experimental results.

Conclusions

Our experiments showed that dual amorphous regions (free amorphous region and constrained amorphous region) coexisted in semicrystalline PET when its f_c^w was moderate. Both lower and upper limits of the f_c^w range increased with increasing T_c for the crystallization from the glassy state. During the physical aging, the whole amount of amorphous phase kept almost constant but some of the free amorphous region gradually evolved into constrained amorphous due to the reduced mobility of molecular segments caused by physical aging. Higher T_{pa} produced a higher rate of physical aging.

Acknowledgment. This work was subsidized by the Special Funds for Major State Basic Research Projects (95-12 and G1999064800).

References and Notes

(1) Jog, J. P. *J. Macromol. Sci., Rev. Macromol. Chem. Phys.* **1995**, *C35*, 531−553.
(2) Schmidt-Rohr, K.; Hu, W.; Zumbulyadis, N. *Science* **1998**, *280*, 714−717.
(3) Schmidt, P. G. *J. Polym. Sci., Part A* **1963**, *1*, 1271−1292.
(4) Sawada, K.; Ishida, Y. *J. Polym. Sci., Polym. Phys.* **1975**, *13*, 2247−2250.
(5) Lin, S.-B.; Koenig, J. L. *J. Polym. Sci., Polym. Phys.* **1983**, *21*, 2365−2378.

(6) Santa-Cruz, C.; Baltá-Calleja, F. J.; Zachmann, H. G.; Stribeck, N.; Asano, T. *J. Polym. Sci., Polym. Phys.* **1991**, *29*, 819−824.
(7) Santa-Cruz, C.; Stribeck, N.; Zachmann, H. G.; Baltá-Calleja, F. J. *Macromolecules* **1991**, *24*, 5980−5990.
(8) Rule, R. J.; MacKerron, D. H.; Mahendrasingam, A.; Martin, C.; Nye, T. M. W. *Macromolecules* **1995**, *28*, 8517−8522.
(9) Sakai, Y.; Imai, M.; Kaji, K.; Tsuji, M. *Macromolecules* **1996**, *29*, 8830−8834.
(10) Aref-Azar, A.; Hay, J. N. *Polymer* **1982**, *23*, 1129−1132.
(11) Ito, E.; Tajima, K.; Kobayashi, Y. *Polymer* **1983**, *24*, 877−882.
(12) Bove, L.; D'Aniello, C.; Gorrasi, G.; Guadagno, L.; Vittoria, V. *Polym. Bull. (Berlin)* **1997**, *38*, 579−585.
(13) McGonigle, E.-A.; Daly, J. H.; Gallagher, S.; Jenkins, S. D.; Liggat, J. J.; Olsson, I.; Pethrick, R. A. *Polymer* **1999**, *40*, 4977−4982.
(14) Tribone, J. J.; O'Reilly, J. M.; Greener, J. *Macromolecules* **1986**, *19*, 1732−1739.
(15) Hutchinson, J. M. *Prog. Polym. Sci.* **1995**, *20*, 703−760.
(16) Hutchinson, J. M.; Kovacs, A. J. *J. Polym. Sci., Polym. Phys.* **1976**, *14*, 1575−1590.
(17) Struik, L. C. E. *Physical Aging in Amorphous Polymers and Other Materials*; Elsevier: Amsterdam, 1978.
(18) Struik, L. C. E. *Polymer* **1988**, *29*, 1347−1353.
(19) Petrie, S. E. B. *J. Polym. Sci. A-2* **1972**, *10*, 1255−1272.
(20) O'Reilly, J. M. *J. Appl. Phys.* **1979**, *50*, 6083−6087.
(21) Hodge, I. M. *Macromolecules* **1987**, *20*, 2897−2908.
(22) Hourston, D. J.; Song, M.; Hammiche, A.; Pollock, H. M.; Reading, M. *Polymer* **1996**, *37*, 243−247.
(23) Hutchinson, J. M.; Smith, S.; Horne, B.; Gourlay, G. M. *Macromolecules* **1999**, *32*, 5046−5061.
(24) Song, R.; Zhao, J.; Yang, J.; Linghu, X.; Fan, Q. *Macromol. Chem. Phys.* **2001**, *202*, 512−515.
(25) Zhao, J.; Fan, Q. *Polym. Bull. (Berlin)* **2001**, *47*, 91−97.
(26) D'Esposito, L.; Koenig, J. L. *J. Polym. Sci., Polym. Phys.* **1976**, *14*, 1731−1741.
(27) Ajji, A.; Cole, K. C.; Dumoulin, M. M.; Brisson, J. *Polymer* **1995**, *36*, 4023−4030.
(28) Farrow, G.; Ward, I. M. *Polymer* **1960**, *1*, 330−339.
(29) Ito, E.; Yamamoto, K.; Kobayashi, Y. *Polymer* **1978**, *19*, 39−42.
(30) Qian, R.; Shen, D.; Sun, F.; Wu, L. *Macromol. Chem. Phys.* **1996**, *197*, 1485−1493.
(31) Zhang, W.; Shen, D. *Polym. J.* **1998**, *30*, 311−314.
(32) Wang, Y.; Shen, D.; Qian, R. *J. Polym. Sci., Polym. Phys.* **1998**, *36*, 783−788.
(33) Wang, Y.; Lu, J.; Shen, D. *Polym. J.* **2000**, *32*, 560−566.
(34) Schael, G. W. *J. Appl. Polym. Sci.* **1966**, *10*, 901−915.
(35) Groeninckx, G.; Berghmans, H.; Smets, G. *J. Polym. Sci., Polym. Phys.* **1976**, *14*, 591−602.
(36) Struik, L. C. E. *Polymer* **1987**, *28*, 1521−1533, 1534−1542; **1989**, *30*, 799−814; 815−830.
(37) Read, B. E.; Tomlins, P. E.; Dean, G. D. *Polymer* **1990**, *31*, 1204−1215.
(38) Vigier, G.; Tatibouet, J.; Benatmane, A.; Vassoille, R. *Colloid Polym. Sci.* **1992**, *270*, 1182−1187.
(39) Vigier, G.; Tatibouet, J. *Polymer* **1993**, *34*, 4257−4266.
(40) Montserrat, S.; Cortés, P. *J. Mater. Sci.* **1995**, *30*, 1790−1793.
(41) Diego, J. A.; Caòadas, J. C.; Mudarra, M.; Belana, J. *Polymer* **1999**, *40*, 5355−5363.
(42) Itoyama, K. *Polymer* **1994**, *35*, 2117−2122.
(43) Zhao, J.; Song, R.; Zhang, Z.; Linghu, X.; Zheng, Z.; Fan, Q. *Macromolecules* **2001**, *34*, 343−345.
(44) Siegmann, A.; Turi, E. *J. Macromol. Sci., Phys.* **1974**, *B10*, 689−708.
(45) Jabarin, S. A. *Polym. Eng. Sci.* **1989**, *29*, 1259−1264.
(46) Brunacci, A.; Cowie, J. M. G.; Ferguson, R.; Gómez-Ribelles, J. L.; Vidaurre-Garayo, A. *Macromolecules* **1996**, *29*, 7976−7988.
(47) Hristov, H. A.; Schultz, J. M. *J. Polym. Sci., Polym. Phys.* **1990,** *28*, 1647−1663.
(48) Boyer, R. F. *Macromolecules* **1973**, *6*, 288−299.
(49) Boyer, R. F. *J. Macromol. Sci., Phys.* **1973**, *B8*, 503−537.
(50) Hay, J. N. *Pure Appl. Chem.* **1995**, *67*, 1855−1858.
(51) Mayhan, K. G.; James, W. J.; Bosch, W. *J. Appl. Polym. Sci.* **1965**, *9*, 3605−3616.
(52) Van-Antwerpen, F.; Van-Krevelen, D. W. *J. Polym. Sci., Polym. Phys.* **1972**, *10*, 2423−2435.
(53) Shinn, T.; Lin, C. *J. Appl. Polym. Phys.* **1993**, *49*, 1093−1105.
(54) Ou, C.; Lin, C. *J. Appl. Polym. Phys.* **1996**, *61*, 1447−1454.
(55) Zhu, P.; Ma, D. *Eur. Polym. J.* **1997**, *33*, 1817−1818.
(56) Tant, M. R.; Wilkes, G. L. *J. Appl. Polym. Phys.* **1981**, *26*, 2813−2825.
(57) Cheng, S. Z. D.; Cao, M.-Y.; Wunderlich, B. *Macromolecules* **1986**, *19*, 1868−1876.

MA011333Z